# Seismic Analysis of Wood-Stone Structures with Three Degree of Freedom Systems

Gangzhu Sun,[a] Guosen Zhou,[a,b] and Panxu Sun [a,*]

Wood and stone have different damping ratios. The seismic analysis of wood-stone structures is important. The vertical wood-stone structure is regarded as a three degree of freedom system. Based on Caughey damping model of substructures, the whole damping matrix was constructed. Then combined with Newmark-$\beta$ method, a numerical method was proposed to calculate dynamic responses of wood-stone structures. Numerical results showed that the seismic performance of wood-stone structures was stronger than that of stone structures, and it was weaker than that of wood structures. During the process of earthquake action, the middle wood substructure can obviously improve seismic performance of the wood-stone structure. The bottom structure has greater stiffness, but weaker seismic performance.

*DOI: 10.15376/biores.21.1.178-187*

*Keywords: Seismic response; Wood-stone; Numerical method; Substructures; Caughey damping model*

*Contact information: a: School of Civil Engineering, Zhengzhou University, Zhengzhou, 450001, China; b: China Construction Fifth Engineering Bureau, Changsha, 410004, China;*
**Corresponding author: panxusun@zzu.edu.cn*

## INTRODUCTION

Under the action of earthquake waves, some ancient building structures have suffered certain degrees of damage (Huan *et al.* 2025). Specifically, some ancient building structures fully utilized the advantages of natural wood and stone, which were wood-stone structures (Partov *et al.* 2025). He *et al.* (2025) statistically analyzed the field damage data from destructive earthquakes and identified seismic damage characteristics of wood-stone structures. Sayin *et al.* (2025) analyzed the seismic performance assessment and restoration of the Karacakaya Mosque that has a wood-stone structure. Shen *et al.* (2021) studied the seismic resistance of wood-stone frames in a Chinese traditional village dwelling. However, the seismic performance evaluation of these wood-stone structures is mostly based on on-site and experimental analysis. The numerical analysis of seismic performance is difficult to evaluate for wood-stone structures. The reason is that wood and stone have different damping characteristics.

Some Chinese theater buildings and temples in scenic spots are made of wood-stone structures. The top structure is a stone substructure. The middle structure is a wood substructure, and the bottom structure is a stone substructure. The wood-stone structures are non-proportional damping systems. The Rayleigh damping model can be applied for non-proportional damping systems (Mogi *et al.* 2022). The Rayleigh damping model usually only considers the influence of certain two-vibration modes, which is suitable for simplification of structures into two degree of freedom systems. However, the wood-stone structure is essentially a three degree of freedom system, having materials with different damping characteristics (Huang *et al.* 2015). Sivandi-Pour *et al.* (2016) analyzed the seismic performance of the hybrid structure containing concrete, steel, and transitional storeys based on block damping matrix of the three degree of freedom system. Kaveh and Ardebili (2022) analyzed seismic behavior for steel-concrete-soil structures by aid of equivalent damping ratio. The equivalent damping ratio is beneficial for the calculation process, but it cannot consider the non-proportional damping characteristics of the system. The Caughey damping model based on the Rayleigh damping model can be further extended for non-proportional damping structures (Volpi and Ritto 2021). However, the damping matrix of wood-stone structures is difficult to determine based on Caughey damping model (Richiedei *et al.* 2021). Therefore, the block damping model can be further applied to wood-stone structures. It is important to construct a calculation method of dynamic responses for wood-stone structures.

The aim of this study was to analyze the seismic performance of wood-stone structures. Some traditional wood-stone structures can be regarded as a three degree of freedom system. Based on the improved Caughey damping model of substructures, all the natural frequencies can be considered, and the damping matrix can be further obtained. Combined with Newmark-$\beta$ method, a numerical method was proposed to calculate the dynamic responses of wood-stone structures. Then wood structures, stone structures and wood-stone structures were compared and analyzed. Based on the seismic indexes, the seismic performance of wood-stone structures was quantitatively analyzed.

## NUMERICAL METHOD FOR SEISMIC RESPONSES OF WOOD-STONE STRUCTURES WITH THREE DEGREE OF FREEDOM SYSTEM

Taking Chinese theatre buildings as an example (as shown in Fig. 1), the material of top and bottom substructures is made of stone, and the material of middle substructure is wood. Therefore, the wood-stone structure can be regarded as a three degree of freedom system in dynamic analysis.

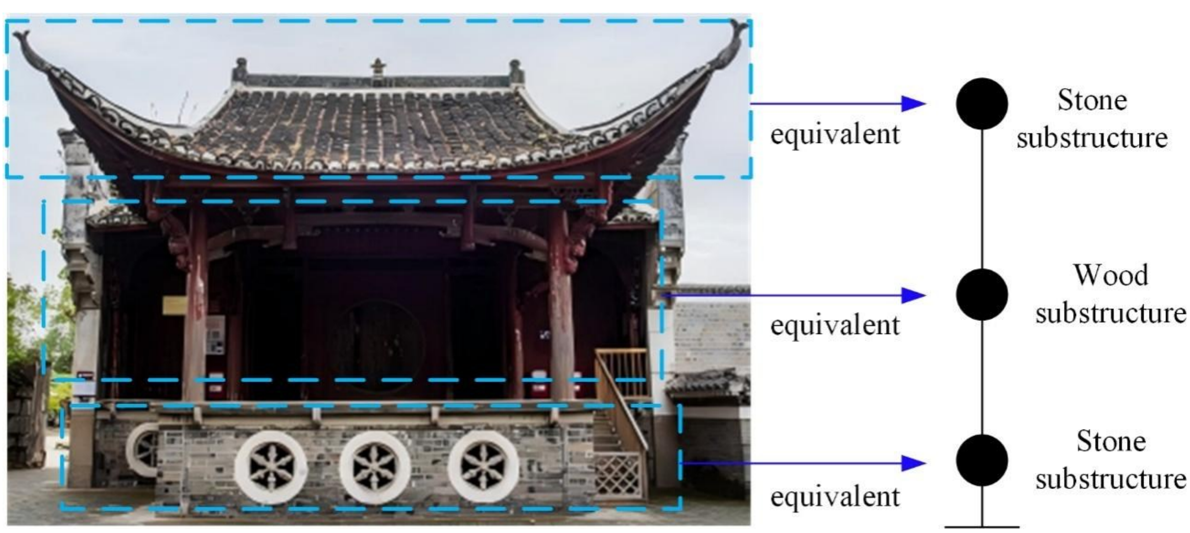


**Fig. 1.** Simplified mechanical model of the Chinese theatre building

The time-domain motion equation can be expressed as

$$\mathbf{M}\ddot{\mathbf{x}}(t)+\mathbf{C}\dot{\mathbf{x}}(t)+\mathbf{K}\mathbf{x}(t)=\mathbf{f} \tag{1}$$

where $\mathbf{M}$ is the mass (kg) matrix; $\mathbf{K}$ is the stiffness (N/m) matrix; $\mathbf{C}$ is the damping matrix; $\mathbf{x}(t)$ is the structural displacement vector; and $\mathbf{f}$ is the external excitation matrix.

The damping matrix consists of the damping matrices of the three substructures, which can be summed as,

$$\mathbf{C}=\mathbf{C}_{\mathrm{t}}+\mathbf{C}_{\mathrm{m}}+\mathbf{C}_{\mathrm{b}} \tag{2}$$

where $\mathbf{C}_{\mathrm{t}}$ is the damping matrix of the top substructure; $\mathbf{C}_{\mathrm{m}}$ is the damping matrix of the middle substructure; and $\mathbf{C}_{\mathrm{b}}$ is the damping matrix of the bottom substructure.

Based on modal analysis method, the natural frequencies of the three degrees of freedom system are as follows:

$$\varpi=\begin{bmatrix}\varpi_1 & \varpi_2 & \varpi_3\end{bmatrix} \tag{3}$$

The traditional Rayleigh damping model can only analyze the two natural frequencies, which means that it cannot analyze all natural frequencies. Here, the Caughey damping model was adopted, such that the damping matrices of the three substructures can be expressed as

$$\begin{cases}\mathbf{C}_{\mathrm{t}}=\alpha_{\mathrm{t}}\mathbf{M}_{\mathrm{t}}+\beta_{\mathrm{t}}\mathbf{K}_{\mathrm{t}}+\gamma_{\mathrm{t}}\mathbf{K}_{\mathrm{t}}\mathbf{M}_{\mathrm{t}}^{-1}\mathbf{K}_{\mathrm{t}}\\ \mathbf{C}_{\mathrm{m}}=\alpha_{\mathrm{m}}\mathbf{M}_{\mathrm{m}}+\beta_{\mathrm{m}}\mathbf{K}_{\mathrm{m}}+\gamma_{\mathrm{m}}\mathbf{K}_{\mathrm{m}}\mathbf{M}_{\mathrm{m}}^{-1}\mathbf{K}_{\mathrm{m}}\\ \mathbf{C}_{\mathrm{b}}=\alpha_{\mathrm{b}}\mathbf{M}_{\mathrm{b}}+\beta_{\mathrm{b}}\mathbf{K}_{\mathrm{b}}+\gamma_{\mathrm{b}}\mathbf{K}_{\mathrm{b}}\mathbf{M}_{\mathrm{b}}^{-1}\mathbf{K}_{\mathrm{b}}\end{cases} \tag{4}$$

where $\alpha_{\mathrm{t}}$, $\beta_{\mathrm{t}}$ and $\gamma_{\mathrm{t}}$ are damping coefficients of top substructure; $\mathbf{M}_{\mathrm{t}}$ is the mass matrix of the top substructure; $\mathbf{K}_{\mathrm{t}}$ is the stiffness matrix of the top substructure; $\alpha_{\mathrm{m}}$, $\beta_{\mathrm{m}}$ and $\gamma_{\mathrm{m}}$ are the damping coefficients of the middle substructure; $\mathbf{M}_{\mathrm{m}}$ is the mass matrix of the middle substructure; $\mathbf{K}_{\mathrm{m}}$ is the stiffness matrix of the middle substructure; $\alpha_{\mathrm{b}}$, $\beta_{\mathrm{b}}$ and $\gamma_{\mathrm{b}}$ are the damping coefficients of bottom substructure; $\mathbf{M}_{\mathrm{b}}$ is the mass matrix of the bottom substructure; and $\mathbf{K}_{\mathrm{b}}$ is the stiffness matrix of the bottom substructure.

The mass matrix was selected as a diagonal matrix, which is

$$\mathbf{M}=\begin{bmatrix}m_{\mathrm{t}} & 0 & 0\\ 0 & m_{\mathrm{m}} & 0\\ 0 & 0 & m_{\mathrm{b}}\end{bmatrix} \tag{5}$$

Based on Eq. 5, the Caughey damping model was improved. The inverse matrices of the mass matrices for the three substructures are generalized inverse matrices. These matrices can be expressed as

$$\mathbf{M}_{\mathrm{t}}=\begin{bmatrix}1/m_{\mathrm{t}} & 0 & 0\\ 0 & 0 & 0\\ 0 & 0 & 0\end{bmatrix},\ \mathbf{M}_{\mathrm{m}}=\begin{bmatrix}0 & 0 & 0\\ 0 & 1/m_{\mathrm{m}} & 0\\ 0 & 0 & 0\end{bmatrix},\ \mathbf{M}_{\mathrm{b}}=\begin{bmatrix}0 & 0 & 0\\ 0 & 0 & 0\\ 0 & 0 & 1/m_{\mathrm{b}}\end{bmatrix} \tag{6}$$

The solutions of damping coefficients of top substructure are taken as example. These damping coefficients satisfy Eq. 7, namely

$$\frac{\alpha_{\mathrm{t}}}{\varpi}+\beta_{\mathrm{t}}\varpi+\gamma_{\mathrm{t}}\varpi^{3}=2\xi_{\mathrm{s}} \tag{7}$$

where $\xi_{\mathrm{s}}$ is damping ratio of stone material.

The three natural frequencies are substituted into Eq. 7, which is rewritten as

$$\begin{cases}\dfrac{\alpha_{\mathrm{t}}}{\varpi_1}+\beta_{\mathrm{t}}\varpi_1+\gamma_{\mathrm{t}}\varpi_1^{3}=2\xi_{\mathrm{s}}\\ \dfrac{\alpha_{\mathrm{t}}}{\varpi_2}+\beta_{\mathrm{t}}\varpi_2+\gamma_{\mathrm{t}}\varpi_2^{3}=2\xi_{\mathrm{s}}\\ \dfrac{\alpha_{\mathrm{t}}}{\varpi_3}+\beta_{\mathrm{t}}\varpi_3+\gamma_{\mathrm{t}}\varpi_3^{3}=2\xi_{\mathrm{s}}\end{cases} \tag{8}$$

To solve Eq. 8, these damping coefficients are obtained as

$$\begin{cases}\alpha_{\mathrm{t}}=2\xi_{\mathrm{s}}\dfrac{\varpi_1\varpi_2}{\varpi_1+\varpi_2}\left[1-\dfrac{\varpi_1\varpi_2}{(\varpi_2+\varpi_3)(\varpi_1+\varpi_3)}\right]\\ \beta_{\mathrm{t}}=\dfrac{2\xi_{\mathrm{s}}}{\varpi_1}\left[1+\dfrac{\varpi_1^{3}-\varpi_2^{2}\varpi_3-\varpi_1\varpi_2\varpi_3-\varpi_2\varpi_3^{2}}{(\varpi_1+\varpi_2)(\varpi_2+\varpi_3)(\varpi_1+\varpi_3)}\right]\\ \gamma_{\mathrm{t}}=-2\xi_{\mathrm{s}}\dfrac{1}{(\varpi_1+\varpi_2)(\varpi_2+\varpi_3)(\varpi_1+\varpi_3)}\end{cases} \tag{9}$$

Similarly, these damping coefficients of middle and bottom substructures are obtained as,

$$\begin{cases}\alpha_{\mathrm{m}}=2\xi_{\mathrm{w}}\dfrac{\varpi_1\varpi_2}{\varpi_1+\varpi_2}\left[1-\dfrac{\varpi_1\varpi_2}{(\varpi_2+\varpi_3)(\varpi_1+\varpi_3)}\right]\\ \beta_{\mathrm{m}}=\dfrac{2\xi_{\mathrm{w}}}{\varpi_1}\left[1+\dfrac{\varpi_1^{3}-\varpi_2^{2}\varpi_3-\varpi_1\varpi_2\varpi_3-\varpi_2\varpi_3^{2}}{(\varpi_1+\varpi_2)(\varpi_2+\varpi_3)(\varpi_1+\varpi_3)}\right]\\ \gamma_{\mathrm{m}}=-2\xi_{\mathrm{w}}\dfrac{1}{(\varpi_1+\varpi_2)(\varpi_2+\varpi_3)(\varpi_1+\varpi_3)}\end{cases} \tag{10}$$

$$\begin{cases}\alpha_{\mathrm{b}}=2\xi_{\mathrm{s}}\dfrac{\varpi_1\varpi_2}{\varpi_1+\varpi_2}\left[1-\dfrac{\varpi_1\varpi_2}{(\varpi_2+\varpi_3)(\varpi_1+\varpi_3)}\right]\\ \beta_{\mathrm{b}}=\dfrac{2\xi_{\mathrm{s}}}{\varpi_1}\left[1+\dfrac{\varpi_1^{3}-\varpi_2^{2}\varpi_3-\varpi_1\varpi_2\varpi_3-\varpi_2\varpi_3^{2}}{(\varpi_1+\varpi_2)(\varpi_2+\varpi_3)(\varpi_1+\varpi_3)}\right]\\ \gamma_{\mathrm{b}}=-2\xi_{\mathrm{s}}\dfrac{1}{(\varpi_1+\varpi_2)(\varpi_2+\varpi_3)(\varpi_1+\varpi_3)}\end{cases} \tag{11}$$

where $\xi_{\mathrm{w}}$ is damping ratio of wood material.

Then these damping coefficients of substructures were substituted into Eqs. 2 and 4. Equation 1 can be expressed as the explicit equation. However, the damping matrix is not a classically proportional damping matrix. The Newmark-$\beta$ method was adopted to calculate the seismic responses of the wood-stone structure and $\mathbf{x}(t)$ can be obtained (Liu *et al.* 2021). The Newmark-$\beta$ method involves the stability of the calculation process. Here $\beta$ is 0.5 and $\gamma$ is 0.25. The Newmark-$\beta$ method can be converted into the constant average acceleration method. The corresponding calculation process is unconditionally stable.

## NUMERICAL EXAMPLES

The wood structure, stone structure, and wood-stone structure were compared and analyzed. The structural quality and stiffness increased sequentially from top to bottom (Gao *et al.* 2024). The simplified mechanical model was adopted in the numerical example. The mass and stiffness distributions of the three numerical models were the same. But the damping ratios were different. The numerical models are shown in Fig. 2, which are defined as Model A, Model B, and Model C, respectively. The material of Model A is wood and the material of Model B is stone. For Model C, the material of top and bottom substructures is stone, and the material of middle substructure is wood. The damping ratio of stone material is 0.03 (Elmenshawi *et al.* 2010). The damping ratio of wood material is 0.05 (Sun *et al.* 2024).

The mass matrix of top substructure for numerical model is

$$\mathbf{M}_{\mathrm{t}} = \begin{bmatrix} 1000 & 0 & 0 \\ 0 & 0 & 0 \\ 0 & 0 & 0 \end{bmatrix} \mathrm{kg} \tag{12}$$

The stiffness matrix of top substructure for numerical model is

$$\mathbf{K}_{\mathrm{t}} = \begin{bmatrix} 0.5 & -0.5 & 0 \\ -0.5 & 0.5 & 0 \\ 0 & 0 & 0 \end{bmatrix} \times 10^5 \, \mathrm{N/m} \tag{13}$$

The mass matrix of middle substructure for numerical model is

$$\mathbf{M}_{\mathrm{m}} = \begin{bmatrix} 0 & 0 & 0 \\ 0 & 2000 & 0 \\ 0 & 0 & 0 \end{bmatrix} \mathrm{kg} \tag{14}$$

The stiffness matrix of middle substructure for numerical model is

$$\mathbf{K}_{\mathrm{m}} = \begin{bmatrix} 0 & 0 & 0 \\ 0 & 2 & -2 \\ 0 & -2 & 2 \end{bmatrix} \times 10^5 \, \mathrm{N/m} \tag{15}$$

The mass matrix of bottom substructure for numerical model is

$$\mathbf{M}_\mathrm{b} = \begin{bmatrix} 0 & 0 & 0 \\ 0 & 0 & 0 \\ 0 & 0 & 3000 \end{bmatrix} \mathrm{kg} \tag{16}$$

The stiffness matrix of bottom substructure for numerical model is

$$\mathbf{K}_\mathrm{b} = \begin{bmatrix} 0 & 0 & 0 \\ 0 & 0 & 0 \\ 0 & 0 & 3 \end{bmatrix} \times 10^5\,\mathrm{N/m} \tag{17}$$

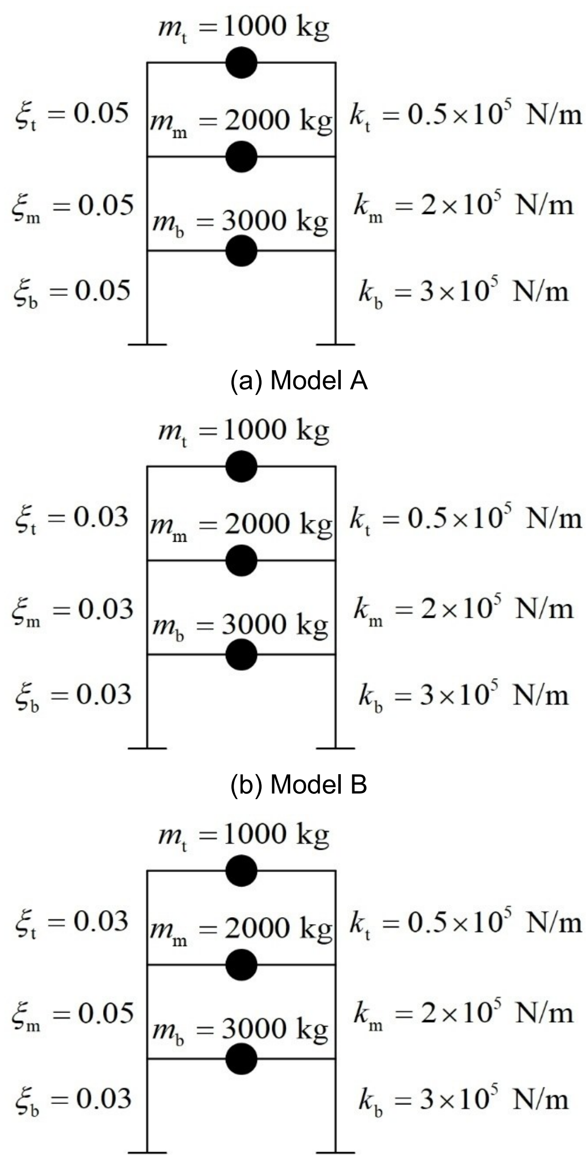


(a) Model A

(b) Model B

(c) Model C

**Fig. 2.** Schematic diagram of the structures with different material

The El Centro earthquake wave is a classic seismic wave, which is usually used in seismic analysis of structures. Here the El Centro earthquake wave was adopted. The acceleration recording is shown in Fig. 3a, and the corresponding Fourier spectrum is shown in Fig. 3b. The peak acceleration was 210.10 mm/s$^2$ and the earthquake duration was 20.48 s. The natural frequencies of Model A, Model B and Model C were 5.0856 rad/s, 9.1139 rad/s and 15.2558 rad/s. Figure 3b shows that the main frequency range of El Centro earthquake wave was 0 to 50 rad/s. El Centro earthquake waves were able to cover all natural frequencies of numerical models.

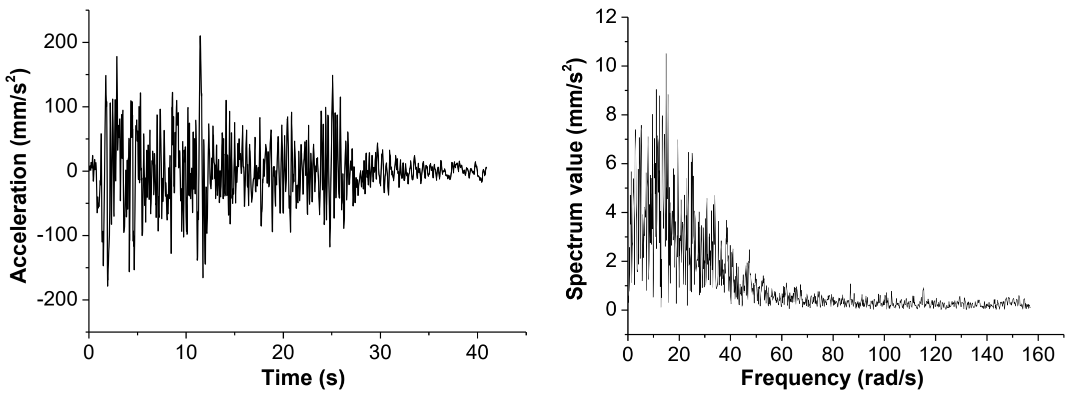


**(a)** Acceleration time-history **(b)** Fourier spectrum

**Fig. 3.** Acceleration time-history and Fourier spectrum of El Centro earthquake wave

Model A and Model B are classical damping systems, and the traditional modal superposition method was used to calculate the seismic responses (Bracci *et al.* 1997). The proposed method was used to calculate the seismic responses of Model C. The peak value of top displacement and peak story drift were selected as indexes, which were used to analyze the difference of the three numerical models. The comparisons of seismic indexes for different numerical models are shown in Table 1.

Compared with Model C, the relative difference of peak value of top displacement for Model A was −14.11%, and the relative difference of peak value of top displacement for Model B was 7.46%. The peak story drifts of Model A were smaller than those of Model C. The peak story drifts of Model B were greater than those of Model C. The results show that the seismic performance of wood-stone structures was stronger than that of stone structures, and it was weaker than that of wood structures. The reason is that the damping ratio of wood material is greater than that of stone material. Besides, compared with Model B and Model C, the relative differences of peak story drifts of the first floor and third floor were less than 10%, and the relative difference of peak story drifts of the second floor was greater than 10%.

During the process of earthquake action, the middle wood substructure can obviously improve seismic performance of the wood-stone structure. The bottom substructure has greater stiffness, but weaker seismic performance. In the subsequent reinforcement, it is necessary to enhance the seismic resistance of the bottom substructure.

**Table 1.** Comparisons of Seismic Responses for Different Numerical Models

| | Model A | Model B | Model C |
|---|---|---|---|
| Peak value of top displacement (mm) | 24.17 | 30.24 | 28.14 |
| Relative difference (%) | –14.11 | 7.46 | — |
| Peak story drift of the first floor (mm) | 5.14 | 6.67 | 6.30 |
| Relative difference (%) | –18.41 | 5.87 | — |
| Peak story drift of the second floor (mm) | 6.08 | 8.10 | 7.12 |
| Relative difference (%) | –14.61 | 13.76 | — |
| Peak story drift of the third floor (mm) | 14.73 | 17.92 | 17.01 |
| Relative difference (%) | –13.40 | 5.35 | — |

## CONCLUSIONS

1. The vertical wood-stone structure can be regarded as a three degree of freedom system. To solve the problem of difficulty in constructing damping matrix, an improved Caughey damping model based on the generalized damping matrix and block damping model of substructures was proposed. Based on the improved Caughey damping model of substructures, the non-proportional damping characteristics and all the natural frequencies were considered. Then the explicit dynamic equation of wood-stone structures was constructed. By aid of Newmark-$\beta$ method, a numerical method was developed to calculate the dynamic responses of wood-stone structures.

2. The damping ratio of wood material is greater than that of stone material. Based on the peak value of top displacement and peak story drift, the performance of wood-stone structures was quantitatively analyzed. The seismic performance of wood-stone structures was found to be stronger than that of stone structures, and it was weaker than that of wood structures. During the process of earthquake action, the middle wood substructure can obviously improve seismic performance of the wood-stone structure. The bottom substructure has greater stiffness, but weaker seismic performance. In the subsequent reinforcement, it is necessary to enhance the seismic resistance of the bottom substructure.

In further work, the optimization strategy of enhancing the damping performance of the bottom substructure will be further studied for wood-stone structures. Besides, the seismic performance of wood-stone structures is related to the excellent frequency range of seismic waves. Due to seismic waves with different frequency characteristics, the dynamic performance of wood-stone structures needs to be further studied.

## ACKNOWLEDGMENTS

This work was supported by the National Natural Science Foundation of China (Grant No. 52208322), China Postdoctoral Science Foundation (Grant No. 2025T180893), Science and Technology Research Project of Henan Province (Grant No. 252102321013), Young Elite Scientists Sponsorship Program by Henan Association for Science and Technology (Grant No. 2025HYTP009), and Postdoctoral Research Foundation of Henan Province (Grant No. HN2025034).

## REFERENCES CITED

Bracci, J. M., Kunnath, S. K., and Reinhorn, A. M. (1997). "Seismic performance and retrofit evaluation of reinforced concrete structures," *Journal of Structural Engineering* 123(1), 3-10. DOI: 10.1061/(ASCE)0733-9445(1997)123:1(3)

Elmenshawi, A., Sorour, M., Mufti, A., Jaeger, L.G., and Shrive, N. (2010). "Damping mechanisms and damping ratios in vibrating unreinforced stone masonry," *Engineering Structures* 32(10), 3269-3278. DOI: 10.1016/j.engstruct.2010.06.016

Gao, X., Tan, Z., and Zhang, J. (2024). "The spatial form of the temple and stage architecture complex in Jinzhong area," *Journal of Shanxi Datong University (Natural Science Edition)* 40(4), 111-115. DOI: 10.3969/j.issn.1674-0874.2024.04.023

He, Z., Guo, H., Zhang, Y., Zhao, Z., Zhang, C., Shi, B., Yang, Y., and Yang, Z. (2025). "Seismic vulnerability model for typical buildings in Sichuan Province, China, based on empirical seismic damage statistics," *Structures* 78, article 109294. DOI: 10.1016/j.istruc.2025.109294

Huan, J., Zhou, X., Guo, X., Wang, W., Ma, D., and He, Y. (2025). "Experimental study and finite element analysis on the seismic performance of ancient architectural kanchuang frame with different impact parameters considered," *BioResources* 20(2), 4304-4329. DOI: 10.15376/biores.20.2.4304-4329

Huang, W., Qian, J., Zhou, Z., and Fu, Q. (2015). "An approach to equivalent damping ratio of vertically mixed structures based on response error minimization," *Soil Dynamics and Earthquake Engineering* 72, 119-128. DOI: 10.1016/j.soildyn.2015.02.008

Kaveh, A., and Ardebili, S. R. (2022). "Equivalent damping ratio for mixed structures including the soil-structure interaction," *Structures* 41, 29-35. DOI: 10.1016/j.istruc.2022.04.090

Liu, Y., Zhang, B., Wang, T., Su, T., and Chen, H. (2021). "Dynamic analysis of multilayer-reinforced concrete frame structures based on NewMark-β method," *Reviews on Advanced Materials Science* 60(1), 1567-577. DOI: 10.1515/rams-2021-0042

Mogi, Y., Nakamura, N. and Ota, A. (2022). " Application of extended Rayleigh damping model to 3D frame analysis evaluation of damping in elastic response history analysis," *Journal of Structural and Construction Engineering* 86(783), 738-748. DOI: 10.1002/2475-8876.12317

Partov, D., Zivaljevic-Luxor, N., Milev, N., Dinev, D., and Lyubenov, L. (2025). "On Bulgarian experience in the repair of damage to listed buildings," *Bauingenieur* 100(4), 80-89. DOI: 10.37544/0005-6650-2025-04-46

Richiedei, D., Tamellin, I., and Trevisani, A. V. (2021). "A homotopy transformation method for interval-based model updating of uncertain vibrating systems," *Mechanism and Machine Theory* 160, article 104288. DOI: 10.1016/j.mechmachtheory.2021.104288

Sayin, B., Akan, A. E., Cosgun, T., Er, A., Samadi, K., Uzdil, O., Basok, G. C., and Örmecioglu, T. O. (2025). "Seismic performance assessment and restoration proposal for the 19th-century Karacakaya Mosque," *Journal of Building Engineering* 108, article 112856. DOI: 10.1016/j.jobe.2025.112856

Shen, Y., Yan, X., Yu, P., Liu, H., Wu, G., and He, W. (2021). "Seismic resistance of timber frames with mud and stone infill walls in a Chinese traditional village dwelling," *Buildings* 11, article 580. DOI: 10.3390/buildings11120580

Sivandi-Pour, A., Gerami, M., and Kheyroddin, A. (2016). "Uniform damping ratio for non-classically damped hybrid steel concrete structures," *International Journal of Civil Engineering* 14, 1-11. DOI: 10.1007/s40999-016-0003-8

Sun, P., Li, K., and Sun, G. (2024). "Seismic performance analysis of wood-steel frame structures," *BioResources* 19(4), 8730-8738. DOI: 10.15376/biores.19.4.8730-8738

Volpi, L. P., and Ritto, T. G. (2021). "Probabilistic model for non-proportional damping in structural dynamics," *Journal of Sound and Vibration* 506, article 116145. DOI: 10.1016/j.jsv.2021.116145

Article submitted: August 17, 2025; Peer review completed: September 18, 2025; Revised version received: October 3, 2025; Accepted: November 5, 2025; Published: November 13, 2025.
DOI: 10.15376/biores.21.1.178-187